Proceedings of the XVII ECSMGE-2019
Geotechnical Engineering foundation of the future
ISBN 978-9935-9436-1-3

doi: 10.32075/17ECSMGE-2019-0193

XVII European Conference
ECSMGE 2019
Reykjavik
on Soil Mechanics
and Geotechnical Engineering

Improved embedded beam with interaction surface

Poutre incorporée améliorée avec surface d'interaction

C.M. Smulders
Adviesbureau voor Bouw Techniek (ABT), Delft, Netherlands

S. Hosseini
Plaxis bv, Delft, Netherlands

R.B.J. Brinkgreve
Delft University of Technology / Plaxis bv, Delft, Netherlands

ABSTRACT: Finite Element Analysis of serviceability limit states (SLS) and bearing capacity (ULS) of piled foundations involves the modelling piles in the soil, including pile-soil interaction. Embedded beams are an efficient way to model multiple piles for complex practical applications. Following initial work of Sadek & Shahrour (2004) on embedded beam elements, Turello et al (2016a,b) introduced a new embedded beam formulation with interaction surface to overcome mesh-dependence and to improve the behaviour under lateral loading. The proposed paper describes an improvement and further evolution of the embedded beam with interaction surface for practical applications. The element has been implemented in the PLAXIS finite element software, compared with previous implementations and validated against pile load test data. The paper will show that the results of the new implementation are more accurate and less mesh-dependent than the previous implementation and the load-displacement performance is much closer to the actual pile response; both in axial loading and in lateral loading.

RÉSUMÉ: L'analyse par éléments finis des états limites de service (SLS) et de la capacité portante (ULS) des fondations sur pieux implique la modélisation des pieux dans le sol, y compris l'interaction pieu-sol. Les poutres incorporés sont un moyen efficace de modéliser plusieurs pieux pour des applications pratiques complexes. À la suite des travaux initiaux de Sadek et Shahrour (2004) sur les éléments de poutre incorporés, Turello et al (2016a, b) ont présenté une nouvelle formulation de poutre incorporée avec une surface d'interaction permettant de surmonter la dépendance au maillage et d'améliorer le comportement sous chargement latéral. Le document proposé décrit une amélioration et une évolution ultérieure du poutre incorporé avec une surface d'interaction pour des applications pratiques. L'élément a été implémenté dans le logiciel d'éléments finis PLAXIS, comparé aux implémentations précédentes et validé par rapport aux données de test de charge de pieu. Le document montrera que les résultats de la nouvelle mise en œuvre sont plus précis et moins dépendants du maillage que la mise en œuvre précédente et que les performances de déplacement de charge sont beaucoup plus proches de la réponse réelle du pieu; à la fois en chargement axial et en chargement latéral.

Keywords: Numerical modelling, finite element method, embedded beam, pile, pile-soil interaction, end bearing, shaft friction

1 INTRODUCTION

Although piles are essentially one-dimensional objects, the numerical modelling of foundation piles in the ground involves a complex non-linear and three-dimensional (3D) interaction of pile and soil. The straightforward approach is to model the pile as a linear elastic solid object, surrounded by interface elements to model the soil-structure interaction, and the soil by means of an appropriate non-linear elastoplastic soil constitutive model. In practical applications, this approach could lead to an extremely large number of elements and, consequently, unacceptable computational cost. To create more efficient numerical models, approaches based on the modelling of piles as beam elements have been proposed, among which the so-called embedded beam element formulation by Sadek & Sharhour (2004). While the original formulation was meant for micro piles, the model was further enhanced for foundation piles by Septanika et al. (2007) by providing realistic shaft resistance and end-bearing, and to overcome premature failure by adding an elastic zone around the beam. In the years thereafter, the embedded beam model was further elaborated and validated for individual foundation piles, pile groups and ground anchors in 2D and 3D under axial compression, tension and lateral loading conditions (Engin et al. 2007, 2008; Lebeau 2008; Tschuchnigg 2009a,b, 2012; Dao 2011; Sluis 2012; Hermans 2014). During those validations it became clear that, the formulation had its limitations, particularly regarding its stress discontinuities, mesh-depencence and less realistic lateral loading behaviour.

To overcome some of these limitations, Turello et al. (2016a,b) developed a different embedded beam element by considering a (virtual) interaction surface to model the pile-soil interaction. This approach is the basis of a further generalization and application as described by Smulders (2018) and this paper.

Section 2 of this paper contains the theoretical and numerical formulation of the generalized model, based on Timoshenko beam theory. Section 3 describes some non-trivial implementational aspects. In Section 4 and 5 the results of the new embedded beam formulation under axial and lateral loading conditions are compared with previous approaches. Finally, Section 6 contains the main conclusions of this study.

2 EMBEDDED BEAM WITH INTERACTION SURFACE

In PLAXIS 3D the embedded beam element is modelled as a 3-noded line element that can cross a 10-noded tetrahedral element representing the soil (Figure 1). However, the line element introduces stress discontinuities and mesh dependence of the model.

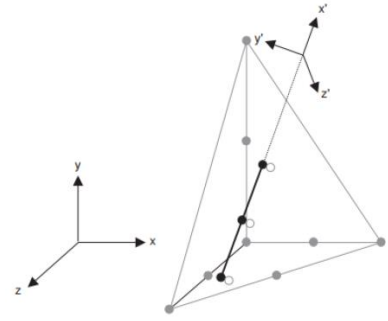

Figure 1. Embedded beam element in PLAXIS 3D as presented by Brinkgreve et al. (2015)

Turello et al. (2016b) proposed an improved embedded beam element which describes the pile-soil interaction at an explicit interaction surface (Figure 2). This explicit interaction surface is meant to solve the aforementioned problems.

In this paper a further extension and improvement of the embedded beam element is proposed. Similar as in the work by Turello et al. (2016b), the pile soil interaction is described at an explicit interaction surface. In order to achieve this, the beam displacements at the beam axis should be mapped to the interaction surface.

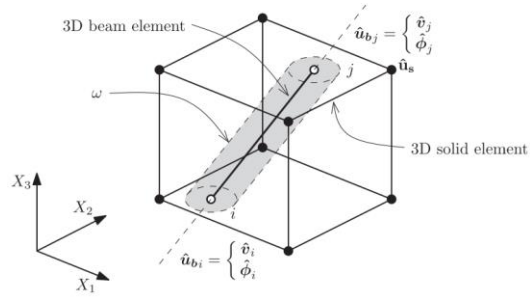

Figure 2. Embedded beam element as proposed by Turello et al. (2016a)

A point on the interaction surface in a global (x,y,z) coordinate system is obtained according to:

$$\boldsymbol{x^0} = \boldsymbol{x_m^0} + \boldsymbol{x_r^0} \quad (1)$$

Where $\boldsymbol{x^0}$ (m) is a vector from the origin to a point on the interaction surface. The vectors $\boldsymbol{x_m^0}$ and $\boldsymbol{x_r^0}$ (m) are indicated in Figure 3. The superscript 0 indicates that the undeformed state is considered, whereas 1 indicates the deformed state.

When a circular beam cross-section is considered, $\boldsymbol{x_r^0}$ can be defined using the pile radius R (m) and orientation angle φ (rad). Subsequently, the beam displacement at a point on the interaction surface can be computed by taking the difference between the deformed and undeformed state.

$$\mathbf{u^b} = \mathbf{x}^1 - \mathbf{x}^0 = \left(\mathbf{x_m^1} - \mathbf{x_m^0}\right) + R\cos\varphi \cdot \left(\mathbf{v_3^1} - \mathbf{v_3^0}\right) + R\sin\varphi \cdot \left(\mathbf{v_2^1} - \mathbf{v_2^0}\right) \quad (2)$$

Where $\boldsymbol{v_2}$ and $\boldsymbol{v_3}$ (-) are local unit vectors (Figure 3). After rewriting and discretization of the beam displacements and rotations using standard interpolation functions $\boldsymbol{N^b}$, the beam displacement vector field $\boldsymbol{u^b}$ (m) at the interaction surface can be expressed in terms of the beam nodal displacements and rotations $\boldsymbol{a^b}$ (m, rad) and a mapping matrix $\boldsymbol{H}$ as follows:

$$\boldsymbol{u^b} = \boldsymbol{H} \cdot \boldsymbol{a^b} \quad (3)$$

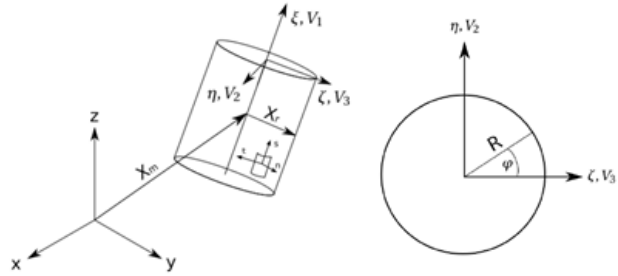

Figure 3. Geometric overview

Where

$$\boldsymbol{H} = \begin{bmatrix} N_1^b & 0 & 0 & \cdots & N_3^b & 0 & 0 & \cdots \\ 0 & N_1^b & 0 & \cdots & 0 & N_3^b & 0 & \cdots \\ 0 & 0 & N_1^b & \cdots & 0 & 0 & N_3^b & \end{bmatrix}$$

$$\begin{bmatrix} 0 & G(1,z) & -G(1,y) & \cdots \\ \cdots -G(1,z) & 0 & G(1,x) & \cdots \\ G(1,y) & -G(1,x) & 0 & \cdots \end{bmatrix}$$

$$\begin{bmatrix} 0 & G(3,z) & -G(3,y) \\ \cdots -G(3,z) & 0 & G(3,x) \\ G(3,y) & -G(3,x) & 0 \end{bmatrix} \quad (4)$$

With

$$G(\alpha,\beta) = RN_\alpha^b\left(\cos\varphi \cdot v_{3\beta}^0 + \sin\varphi \cdot v_{2\beta}^0\right) \quad (5)$$

The soil displacements at the explicit interaction surface $\boldsymbol{u^s}$ (m) are obtained by interpolation within the soil elements that are located on the interaction surface:

$$\boldsymbol{u^s} = \boldsymbol{N^s} \cdot \boldsymbol{a^s} \quad (6)$$

Where $\boldsymbol{a^s}$ (m) is a vector containing the nodal soil displacement values and $\boldsymbol{N^s}$ a matrix containing the interpolation functions.

The relative displacement between the pile and soil $\boldsymbol{\Delta u}$ (m) at the interaction surface can now be computed.

$$\boldsymbol{\Delta u = u^b - u^s = H \cdot a^b - N^s \cdot a^s}$$
$$\boldsymbol{\Rightarrow \Delta u = [H \quad -N^s] \cdot \begin{bmatrix} a^b \\ a^s \end{bmatrix} = B \cdot a^e} \qquad (7)$$

Where $\boldsymbol{B}$ is the deformation matrix, containing the beam and soil mapping/interpolation functions and $\boldsymbol{a^e}$ (m, rad) contains the nodal degrees of freedom of the considered beam and soil elements. In order to describe the pile soil interaction at the interaction surface the relative displacement between pile and soil needs to be transformed to the local (s,n,t) coordinate system. The s-direction is aligned with the beam axis and the n-direction is the outward normal. This transformation can readily be done using two transformation matrices.

$$\boldsymbol{\Delta u_{(s,n,t)} = R_\varphi \, T \Delta u} \qquad (8)$$

Where $\boldsymbol{T}$ describes the transformation from the (x,y,z) coordinate system to the (ξ,η,ζ) coordinate system and $\boldsymbol{R_\varphi}$ describes the subsequent transformation to the (s,n,t) coordinate system (Figure 3). The matrices are given by:

$$\boldsymbol{T} = \begin{bmatrix} v_{1x} & v_{1y} & v_{1z} \\ v_{2x} & v_{2y} & v_{2z} \\ v_{3x} & v_{3y} & v_{3z} \end{bmatrix},$$

$$\boldsymbol{R_\varphi} = \begin{bmatrix} 1 & 0 & 0 \\ 0 & \cos\varphi & \sin\varphi \\ 0 & -\sin\varphi & \cos\varphi \end{bmatrix} \qquad (9)$$

The stresses in the interface between pile and soil at the interaction surface are computed by an incremental stress update:

$$\boldsymbol{\sigma^{t+\Delta t} = \sigma^t + D^e \Delta u^{inc}_{(s,n,t)}} \qquad (10)$$

Where $\boldsymbol{D^e}$ is a matrix containing stiffness terms K_s, K_n and K_t (kN/m^3) and $\boldsymbol{\Delta u^{inc}_{(s,n,t)}}$ (m) is the local relative displacement increment. Integration over an interface element and applying the appropriate local equilibrium conditions leads to:

$$\underbrace{\int_A \boldsymbol{B^T D^e B} \, dA}_{\boldsymbol{K^e}} \cdot \boldsymbol{\Delta a^e_{(s,n,t)} = f^{t+\Delta t}_{ex} - f^t_{in}} \qquad (11)$$

Where $\boldsymbol{K^e}$ is the local interface element stiffness matrix, $\boldsymbol{\Delta a^e_{(s,n,t)}}$ (m) contains the nodal relative displacement increments and $\boldsymbol{f^{t+\Delta t}_{ex}}$ and $\boldsymbol{f^t_{in}}$ (kN) are the external and internal forces at the indicated time-steps.

The contribution of each interface element can readily be transformed to the global coordinate system and assembled, leading to the final system of equilibrium equations of the entire problem. The interface elements at the interaction surface provide the coupling between the pile and soil domains.

3 IMPLEMENTATIONAL ASPECTS

3.1 Number of points on the interaction surface.

The interaction between the pile and soil is evaluated at a certain number of points at the interaction surface. The amount of points that is evaluated has, on the one end, a large influence on the computation time and, on the other hand, on the accuracy of the results. In the current implementation, numerical integrations are preformed using 4 integration points located on the interaction surface. However, the influence of the number of integration points on the accuracy and the performance of the new embedded beam formulation is beyond the scope of this paper.

3.2 Interface properties and plasticity

The element stiffness matrix $\boldsymbol{D^e}$ contains the stiffness terms in the interface along the shaft of the pile. In the existing embedded beam implementation in PLAXIS 3D appropriate stiffness terms have been determined (Septanika et al., 2007; Tschuchnigg, 2012). In the proposed implementation the interface element is no longer a line, but a surface element. The required

adaptation of the stiffness terms for the proposed implementation takes into account this change by dividing the stiffness terms by the perimeter length of the pile, $2\pi R$.

$$K_s = 50 \cdot \frac{G_{soil}}{2\pi R}$$
$$K_n = K_t = \frac{2(1-\nu_i)}{1-2\nu_i} K_s \qquad (12)$$

Where G_{soil} (kN/m^2) is the shear modulus of the soil and ν_i (-) is the Poisson's ratio.

It is proposed to spread the foot resistance over the entire base surface of the pile, whereas in the existing embedded beam implementation the foot resistance works on a single point. The latter results in stress singularities near the foot of the pile, which is largely solved with the implementation of the surface interface. Dividing the existing foot interface stiffness by the cross section area of the pile takes into account the change.

$$K_{foot} = R_{foot} \cdot \frac{G_{soil}}{\pi R} \qquad (13)$$

Where R_{foot} (-) is a reduction factor which should be chosen appropriately.

Slipping of the pile through the soil is taken into account by means of limiting the shear stresses in the interfaces along the shaft, implemented in a plasticity framework:

$$\sqrt{\sigma_s^2 + \sigma_t^2} \leq c_i - \sigma_n^{soil}\, tan\varphi_i \qquad (14)$$

Where σ_s and σ_t (kN/m^2) are local stresses in the interface, σ_n^{soil} (kN/m^2) are normal stresses in the surrounding soil, c_i (kN/m^2) is the cohesion and φ_i (rad) the internal friction angle.

The maximum foot resistance of the pile can be controlled by input parameter F_{max}:

$$\sigma_{foot} = K_{foot} \cdot \Delta u_s \leq \frac{F_{\max}}{\pi R^2} \qquad (15)$$

3.3 Assembly

The proposed formulation of the embedded beam element connects multiple soil elements to one beam element. This results in a large element stiffness matrix and a complex assembly procedure. Therefore a a point wise assembly procedure is proposed to assemble the contributions of each integration point of the interface elements separately to the global stiffness matrix and the internal force vector.

4 COMPARISON IN AXIAL LOADING

The Alzey Bridge pile load test is used to verify the developed embedded beam. The test was carried out near Frankfurt. During the test load cells were installed at the foot of the pile to measure the loads that are carried directly by the pile base, making it possible to differentiate between the pile base capacity and skin traction capacity. The test results and model parameters of the corresponding FE model are presented in Engin et al. (2007). The test considers an axially loaded pile with a diameter of 1.3m and a length of 9.5m. The ground water table is approximately 3.5m below the ground surface. Figure 4 shows the geometry of the test case. The properties of the embedded beam that are used in the PLAXIS model are shown in Table 1.

The first set of calculations have been performed using the direct input of the bearing capacity parameters $T_{skin,max}$ and F_{max}. $T_{skin,max}$ is the maximum traction allowed at the skin of the embedded beam which is considered to be constant along the pile. And F_{max} is the maximum compression force allowed at the foot of the embedded beam.

The bearing capacity of the pile is therefore an input to the analysis and not a result. The values selected for the bearing capacity parameters are selected based on the experimental test and presented in Table 1.

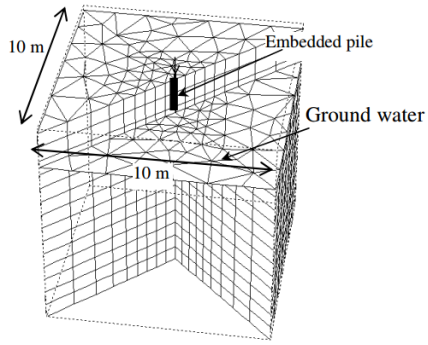

Figure 4. Alzey Bridge pile load test model. (Septanika et al., 2007)

Table 1. Embedded beam parameters for Alzey Bridge model

Parameter	Symbol	Unit
Drainge type	Drained	-
Uniy weight, γ	5	kN/m^3
Young's modulus, E	1.0E7	kN/m^2
Diameter, D	1.3	m
Skin resistance, $T_{skin,\ max}$	201.37	kN/m
Base resistance, F_{max}	1320	kN

Figure 5 and 6 show the results of the first calculation set. The figures also compare the mesh sensitivity of the results. As it was expected the failure load obtained by both the existing and the improved embedded beam elements are in very good agreement with the experimental bearing capacity of 3233 kN. However, it is evident that the existing element shows sensitive and inconsistent results upon mesh refinement whereas the improved element lead to much less mesh sensitive results.

The Alzey Bridge test calculation is repeated with the layer dependent option for the calculation of the skin resistance. Using this option the bearing capacity is obtained as the result of the calculation and not as an input. The results obtained using the existing element and the improved element are shown in Figures 7 and 8. As it can be seen existing element shows mesh sensitive results in terms of both bearing capacity and stiffness. The correctly predicted bearing capacity obtained by the coarse and very fine also seeme more of a coincidence and is not reliable.

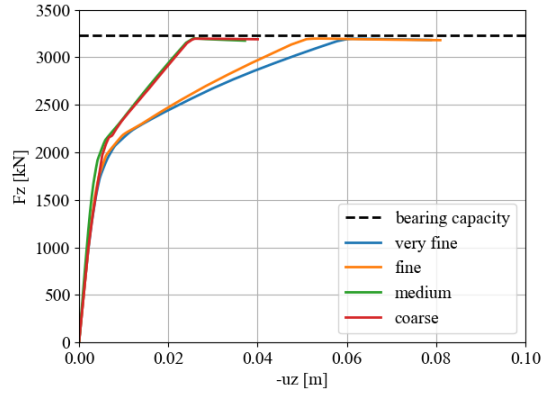

Figure 5. Alzey Bridge pile load test results. Existing embedded beam element with direct bearing capacity inputs.

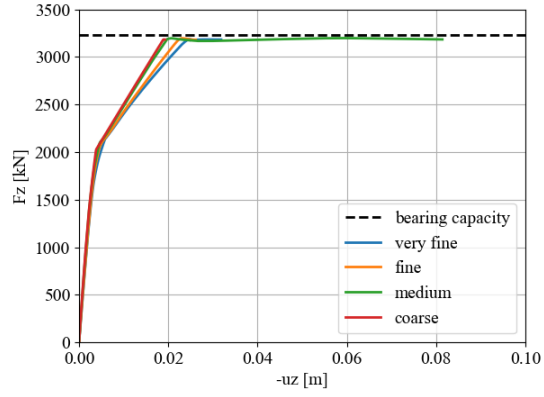

Figure 6. Alzey Bridge pile load test results. Improved embedded beam element with direct bearing capacity inputs.

The new element on the other hand gives more consistent results upon mesh refinement. Unlike the existing element, the new element results in a unique failure load using different meshes, although the bearing capacity is under predicted. It is noted that the layer dependent option uses the soil properties around the embedded pile to extract the strength parameters of the interface. Since the used hardening soil model and its properties are slightly different than the true soil, the difference between the practical and the numerical bearing capacities can be justified.

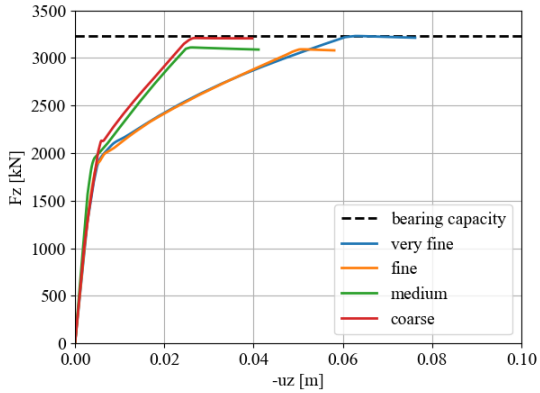

Figure 7. Alzey Bridge pile test results. Existing embedded beam element with layer dependent option.

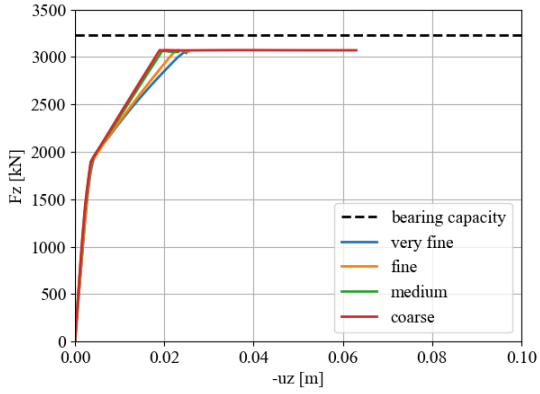

Figure 8. Alzey Bridge pile load test results. Improved embedded beam element with layer dependent option.

5 COMPARISON IN LATERAL LOADING

A simple test case is used to validate the lateral loading behaviour. A disk-shaped pile with a diameter of 0.7 m and length of 1 m is considered (Figure 9). The model parameters of the corresponding FE model can be found in Dao (2011). A pair of lateral forces are applied at the top and the bottom of pile. Because of such a loading it is expected that the compressive stresses develop in the soil in front of the pile. It also causes shear stresses to develop on the sides of the pile. Therefore, a failure mechanism consisting of soil plasticity and soil slippage is expected to happen.

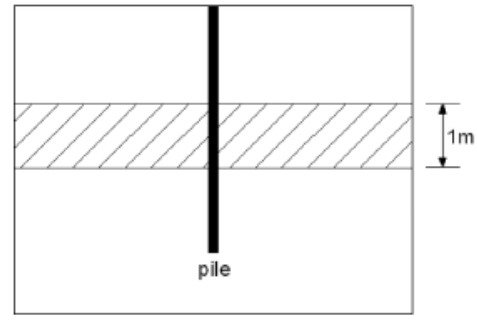

Figure 9. Cross section of the laterally loaded test.

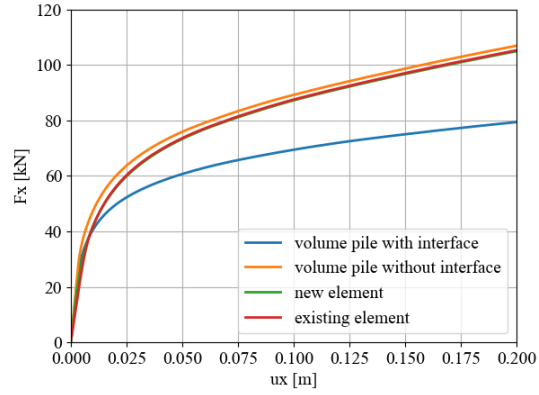

Figure 10. Laterally loaded test results.

Figure 10 compares the obtained results for the laterally loaded test case. The comparison has been made between the new element, existing element and the volume pile method. In the volume pile method, the pile is modelled with volume elements where interface elements are used to capture the soil-structure interaction.

As it can be seen the new embedded beam element shows very close results to the existing element which is not satisfactory. However, the results are comparable with the volume pile results without interface. Considering the reference results (volume pile with interface) it can be concluded that the new element is still not able to capture the soil slippage at the sides of the pile.

6 CONCLUSIONS

Based on previous work by Turello et al. (2016), this paper presents a further generalization, comparison and application of the embedded beam element with interaction surface. This element has been implemented in the PLAXIS Geotechnical Finite Element package. The paper explains the new formulation, provides some implementation details, shows a verification and comparison with the original embedded beam implementation.

From the investigations and applications it is concluded that the new embedded beam element gives more accurate and smoother results in comparison with the original implementation, and the element suffers less from mesh-dependence, at the 'cost' of some extra computation time. It is also concluded that the behaviour in lateral loading is yet sub-optimal. This will be further investigated and improved in future research. Nevertheless, the new embedded beam element is already preferred over the existing implementation.

7 REFERENCES

Brinkgreve, R.B.J., Engin, E., Swolfs, W.M. (2015). Plaxis 3D 2015 manual.

Dao T. (2011). Validation of PLAXIS Embedded Piles for Lateral Loading. MSc thesis. Delft University of Technology

Engin H.K., Septanika E.G., Brinkgreve R.B.J. (2007). Improved embedded beam elements for the modelling of piles. Numerical models in geomechanics (NUMOG X) (eds. Pande & Pietruszczak). London: Taylor & Francis, 475–480

Engin H.K., Septanika E.G., Brinkgreve R.B.J. (2008). Estimation of pile group behavior using embedded piles. Int. Association for Computer Methods and Advances in Geomechanics (ed. Singh). Mumbai, India: IACMAG, 3231–3238

Hermans J.J. (2014). Lateral Loaded Piles – Validation of the Embedded Pile Row in PLAXIS 2D for lateral loading. MSc thesis. Delft University of Technology

Lebeau J.-S. (2008). FE-analysis of piled and piled raft foundations. MSc thesis. Graz University of Technology

Sadek M., Shahrour I. (2004). A three dimensional embedded beam element for reinforced geomaterials. Int. J. for Num. and Anal. Meth. in Geomech. 28: 931–946

Septanika E., Bonnier P.G., Brinkgreve R.B.J., Bakker K.J. (2007). An efficient 3D modeling of (multi) pile-soil interaction. Proceedings Int. Geomechanics Conf., Nessebar, Bulgaria. Sofia: University of mining and geology "St. Ivan Rilski", 67–76

Sluis J.J.M. (2012). Validation of Embedded Pile Row in PLAXIS 2D. MSc thesis. Delft University of Technology

Smulders C.M. (2018). An improved 3D embedded beam element with explicit interaction surface. MSc thesis. Delft University of Technology

Tschuchnigg F. (2009a). Embedded Piles – 1st report. Technische Universität Graz, Computational Geotechnics Group (CCG_IR021_2009)

Tschuchnigg F. (2009b). Embedded Piles – 2nd report. Technische Universität Graz, Computational Geotechnics Group

Tschuchnigg F. (2012). 3D Finite Element Modelling of Deep Foundations Employing an Embedded Pile Formulation. PhD thesis, Technische Universität Graz

Turello D.F., Pinto F., Sanchez P.J. (2016a). Embedded beam element with interaction surface for lateral loading of piles. Int. J. for Num. and Anal. Meth. in Geomech. 40: 568–582

Turello D.F., Pinto F., Sanchez P.J. (2016b). Three dimensional elasto-plastic interface for embedded beam elements with interaction surface for the analysis of lateral loading of piles. Int. J. for Num. and Anal. Meth. in Geomech. 41: 859–879